Fingertip Force Estimation via Inertial and Magnetic Sensors in Deformable Object Manipulation

Mostafa Mohammadi [1,2], Tommaso Lisini Baldi[1,2], Stefano Scheggi [3], and Domenico Prattichizzo [1,2]

Abstract— Fingertip contact forces are of utmost importance in evaluating the quality of the human grasp. However, measuring such forces during object manipulation is not a trivial task. In this paper, we propose a novel method to estimate the fingertip contact forces in grasping deformable objects with known shape and stiffness matrix. The proposed approach uses a sensing glove instrumented with inertial and magnetic sensors. Data obtained from the accelerometers and gyroscopes placed on the distal phalanges are used to determine when the fingers establish contacts with the object. The sensing glove is used to estimate the configuration of the hand and the deformation of the object at each contact with the fingertips of the human hand. The force exerted by each fingertip is obtained by multiplying the stiffness matrix of the object and the vector of object's local deformation in the contact point. Extensive simulations have been performed in order to evaluate the robustness of the proposed approach to noisy measurements, and uncertainties in human hand model. In order to validate the proposed approach, experimental validations with a virtual object have been performed. A haptic device was used to generate the contact forces with the virtual object and accurately measure the forces exerted by the users during the interaction.

I. INTRODUCTION

Contact forces determine the quality of a grasp in object manipulation for human and robotic hands. The knowledge of the fingertip contact forces in grasping and manipulating an object can be useful in a variety of research areas such as: anatomical study [1], brain researches [2], rehabilitation [3], haptic rendering [4], [5], human action learning [6], human robot interaction [7], and sensorimotor control [8]. For more than two decades data gloves, such as CyberGlove (CyberGlove Systems LLC, USA), based on arrays of resistive bend-sensors were the main reliable solution for hand gesture detection [9]. Recently, results in force evaluation using a sensing glove made by pressure sensors have been presented in [10], where the authors show a flexible and stretchable fabric-based tactile data glove to measure the

Fig. 1. Inertial and magnetic sensors can be used to estimate fingertip contact forces in grasping deformable objects: (top) a daily grasp situation, (bottom) a sequence of approaching, contact, and squeezing in grasping a deformable object.

[1] Authors are with the Department of Information Engineering and Mathematics, University of Siena, 53100 Siena, Italy. {mohammadi, lisini, prattichizzo}@diism.unisi.it
[2] Authors are with the Department of Advanced Robotics, Istituto Italiano di Tecnologia, Genova, 16163, Italy. {mostafa.mohammadi, tommaso.lisini, domenico.prattichizzo}@iit.it
[3] Author is with the Surgical Robotics Laboratory, Department of Biomechanical Engineering, MIRA-Institute for Biomedical Technology and Technical Medicine, University of Twente, The Netherlands. s.scheggi@utwente.nl

hand configuration and contact forces. In [11] a low cost simple solution is presented for hand pose reconstruction, while in [8] the authors presented a combination of marker-based vision tracking technique and force/torque sensor for fingertip contact force measurement. In the recent years, researchers tried to solve this problem in different ways. Mascaro et al. [12], [13] utilized changes in fingernail coloration to estimate finger forces using miniature LEDs and photo detectors. A similar study was performed by only using external cameras [14]. Electromyography (EMG) signals of forearm muscles were used to estimate fingers' forces in [15]. However, EMG signals provide a rough estimation of the total force exerted by all the fingers. In [16] the authors used markers on the fingers and force sensors below the finger pads to estimate the position and forces at the contacts. However, force sensors below the finger pads may limit the perception of the contact with the object thus reducing the grasping and manipulation abilities. A method to estimate the interaction forces during the manipulation of an object with known physical parameters was proposed in [17]. The method was based on a RGB-D camera. However,

vision based approaches still suffer from occlusion and need external and non wearable equipments.

By using multi-axes force/torque sensors to measure the contact forces (such as the three degrees of freedom (DoF) approach presented in [18] and the 6-DoF approach presented in [8]) the results might be precise in force measurement. However, heavy equipment and metal parts surrounding the finger pads might cause losing the cutaneous perception significantly. Moreover, multi-axes force/torque sensors still need a tracking system, e.g., Vicon (Vicon Motion Systems, UK) or PhaseSpace (PhaseSpace Motion Capture, USA), to estimate the hand pose and contact points. Data gloves based on inertial and magnetic sensors for hand tracking are presented in [19], [20].

In this paper we propose a new technique for fingertip contact force estimation in grasping deformable objects. The method uses Magnetical, Angular Rate, and Gravity (MARG) sensors to estimate the fingertip contact forces. The proposed system is wearable and allows unlimited workspace. In the proposed approach, we considered negligible rolling and skidding of the fingertips over the object, negligible finger pad deformation compared to the object deformation (hard finger model), and fixed object's pose w.r.t. the palm. We assumed that the stiffness matrix of the object is fixed and does not change with its deformation.

In the proposed approach, the joint angles of the fingers and the orientation of the palm are provided by the MARG sensors of the sensing glove. Then, by considering the kinematic model of the hand, the pose of each fingertip is estimated with respect to the palm [20]. The MARGs are installed on the phalanges and palm (Fig. 1) and measure acceleration, angular rate and magnetic field. Since accelerometer and gyroscope are sensitive to impact, we can use their information to detect the contact events. In fact, when a fingertip touches an object, it is subject to a fast change in the acceleration (and angular velocity), so we can detect the contact time analyzing the raw data of accelerometer and gyroscope. Once a contact event is detected, the position of the corresponding fingertip is considered as the contact frame origin on the object. The axes of the contact frame are defined as follows: two axes are tangent to the object surface and third one (normal axis) points inside the object. For a deformable object with known stiffness matrix, neglecting the change in stiffness matrix due to local deformation, the applied force of each fingertip during the contact is obtained by multiplying the stiffness matrix and the fingertip position vector w.r.t. the contact frame.

Error sources in this method are: hand model errors (including the length of phalanges, and configuration of the hand), MARG measurement errors (including bias and noise), delay in contact event detection, and object's stiffness matrix error. The palm configuration error, i.e., error in the placement of MCP and TM joints, and the phalanges length can cause error in both magnitude and direction of the forces. Thus, an accurate model of the hand improves the accuracy of the estimated forces. Errors in the orientation measurement of each MARG are the most important error sources

of this approach. Therefore, appropriate calibration of the MARGs is important in order to have a better estimation of forces. Delay in contact event detection can also be a reason for error in the direction and amplitude of the estimated forces. It can be reduced by increasing the sampling rate of the sensors. Finally, errors in estimating the object stiffness matrix cause error in the estimation of the fingertip contact forces.

A simulation study has been performed to evaluate the robustness of the proposed approach and to understand how the error sources affect the results of the proposed algorithm. Preliminary experiment with virtual objects were performed in order to validate the proposed approach. An omega.3 (Force Dimension, Switzerland) haptic device was used to provide the user with the contact forces with the object and accurately measure the forces exerted by the user during the interaction.

The rest of the paper is organized as follows. Section II reviews the sensing glove made by inertial and magnetic sensor. Section III explains the fingertip contact force estimation algorithm. Section IV and Section V report the results of simulation and experimental validations. Finally, in Section VI conclusions are drawn and possible subjects of future research are outlined.

II. Hand pose estimation using inertial and magnetic sensors.

In this section we briefly describe the design of the MARG sensing glove, and the algorithms used to estimate the hand's pose. The proposed glove is based on the design presented in [20]. In this preliminary study we instrumented only the thumb and the index finger. The prototype is made by seven MARG sensors: one on the palm, three on the thumb, and three on the index finger as depicted in Fig. 1. Each MARG sensor utilizes a triaxial accelerometer/gyroscope (InvenSense MPU6050) and a triaxial magneto-resistor (Honeywell HMC5883L). The raw data of all the sensors are transmitted to an external PC through serial port at 115200 bps. All the pre-processing and calculations are performed by the external PC.

The hand's pose estimation algorithm assumes a simplified kinematic structure of the hand, with universal joints (two intersecting, orthogonal revolute joints) and planar kinematic chains for the fingers, and neglects the small joint axis movements. Fig. 2 shows the model of the hand used in this work. We assumed that each finger has the metacarpal (MC) bone fixed with respect to the hand frame, and features four DoFs. The trapeziometacarpal (TM) joint of the thumb as well as the metacarpophalangeal (MCP) joint of the index, middle, ring and pinky fingers have two DoFs each (one for adduction/abduction and another for flexion/extension). The MCP and interphalangeal (IP) joints of the thumb, as well as the proximal interphalangeal (PIP) and distal interphalangeal (DIP) joints of the other fingers have one DoF each. The kinematics of each finger is modeled using four parameters encoding angles, two for the base of the finger and two for the remaining joints. The global orientation is parametrized
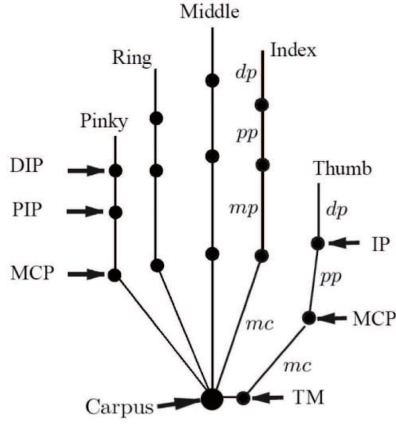
Fig. 2.   Simplified kinematic model of the hand: 4 DoFs for each finger.

Fig. 3.   Hand kinematic parameters: length of the phalanges ($\mathbf{l}_i$), displacement ($\boldsymbol{d}_2$) and rotation ($\mathbf{R}_{0,2}$) of the MCP of the index finger w.r.t. the reference frame of the palm.

using the redundant representation of quaternions. The resulting parametrization encodes 23 DoFs: four DoFs for each finger and three DoFs for the palm rotation. The hand model is represented by 24 parameters: 20 parameters for the fingers (four joint angles for each finger) and a quaternion for the palm.

The hand pose is estimated as follows. In the initial step we estimate the quaternion of each MARG w.r.t. the world reference frame. Then, we determine the rotation of each MARG on the phalanges w.r.t. the one placed on the palm. Finally, the rotation angles of each joint of the finger are estimated. In order to estimate the configuration of each sensor unit w.r.t. the world reference frame, we used a Gauss-Newton method combined with a complementary filter [21]. In order to avoid the *gimbal lock* problem (gimbal lock occurs because the map from Euler angles to rotations is not a covering map) the proposed algorithm uses quaternions to represent rotations. More in detail, at each time frame the gyroscope estimates the angular rates referred to the sensor frame. These values can be integrated over time to obtain an estimation of the quaternion. Concerning accelerometer and magnetometer values, the idea behind the algorithm, is to use the measurement of gravity and earth's magnetic flux obtained from the MARG sensor in order to compute an adjusted measurements of rotation and to limit the effects of drifting in the orientation estimate due to the angular rate integration. The algorithm fuses the quaternion estimated from the accelerometer and magnetometer components with the quaternion estimated from the gyroscope. This operation is provided by a simple filter, known as complementary filter. The filter uses two different gain factors whose sum is one, chosen in order to reduce the noise of each component. Interested readers are referred to [20] for more details.

III. CONTACT FORCE ESTIMATION

The idea behind our algorithm is to use the MARG sensing glove to estimate the hand pose and contemporary estimate the contact forces by detecting if and which finger enters in contact with the object. As a finger comes in contact with the object, the algorithm updates and rearrange the contact frames, positions, and forces vectors.
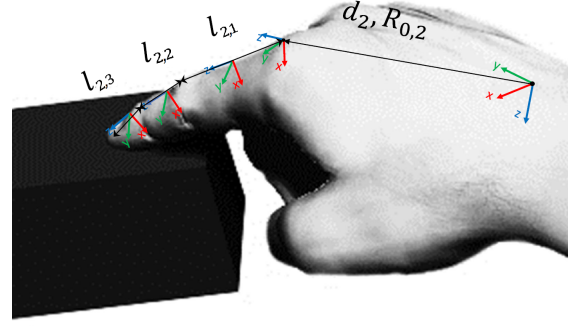
The hand kinematic parameters $\boldsymbol{l}_i = [l_{i,1}, l_{i,2}, l_{i,3}] \in \mathbb{R}^3$ for $i = 1, ..., 5$ represent the length of metacarpal, proximal and distal phalanges of the thumb, and proximal, middle, and distal phalanges for index, middle, ring, and pinky fingers, respectively (thumb is indicated by $i = 1$, and pinky is indicated by $i = 5$). Let the hand configuration parameters $\mathbf{R}_{0,i} \in \mathbf{SO}(3)$, and $\boldsymbol{d}_i \in \mathbb{R}^3$ be the rotation matrix and the translation vector of the TM (for the thumb) and MCP (for index, middle, ring, and pinky fingers) w.r.t. the palm (Carpus), respectively (see Fig. 2, and Fig. 3). We indicate with $\boldsymbol{\theta}_i(t) = [\theta_{i,1}(t), \theta_{i,2}(t), \theta_{i,3}(t), \theta_{i,4}(t)] \in \mathbb{R}^4$ the vector of the joint angles of each finger, where $\theta_{i,1}(t)$ shows the adduction-abduction movement, and $\theta_{i,2}(t), \theta_{i,3}(t)$, and $\theta_{i,4}(t)$ show the flexion-extension movements of TM, MCP, and IP for the thumb, and MCP, PIP, and DIP for the other fingers, respectively. The pose of each finger pads is shown by pair $(\mathbf{R}_i(t), \mathbf{p}_i(t))$, where $\mathbf{R}_i(t) \in \mathbf{SO}(3)$ is the rotation matrix of the finger pad w.r.t. the palm, and $\mathbf{p}_i(t) = [p_i^x(t), p_i^y(t), p_i^z(t)]^\top \in \mathbb{R}^3$ is the position vector of the finger pad w.r.t. the palm. The pose of each finger pad can be obtained from the simple kinematic chain of the finger.

In order to detect the contact events, the algorithm monitors the data from the accelerometers and gyroscopes placed on the distal phalanges. Once the norm of the acceleration and angular velocity of a distal phalanx are above certain thresholds a contact is detected. Let us define the contact event signal $\alpha_i(t) \in \{0, 1\}$, $i = 1, ..., 5$ for each finger as follows:

$$\alpha_i(t) = \begin{cases} 1 & \text{if } \|\mathbf{a}_i\| > a_{th} \quad \& \quad \|\mathbf{g}_i\| > g_{th} \\ 0 & \text{otherwise} \end{cases}$$

where $\|\mathbf{a}_i\|$, and $\|\mathbf{g}_i\|$ are the norm of acceleration and angular rate for the distal phalanges of each finger, and $a_{th} \in \mathbb{R}^+$, and $g_{th} \in \mathbb{R}^+$ are the thresholds. These values might depend on the motion profile of the finger and on the stiffness of the object. Thus, we need to find them experimentally. Let $t_{c,i} \in \mathbb{R}^+$ be the time instant in which $\alpha_i(t) = 1$, we define

a new contact frame $C_i = \langle O_i, \mathbf{x}_i, \mathbf{y}_i, \mathbf{z}_i \rangle$ where O_i is the origin of the contact frame, whose distance from the palm is equal to $\mathbf{p}_i(t_{c,i})$, two of its axes ($\mathbf{y}_i$ and $\mathbf{z}_i$) are tangent to the surface of the object, and $\mathbf{x}_i$ is the normal component of the coordinate frame pointing inside the object. Let $\mathbf{R}_i(t_{c,i})$ be the rotation matrix of such coordinate frame w.r.t. palm. The position of each fingertip w.r.t. the new contact frame $\mathbf{p}_{c,i}(t) = [p_{c,i}^x(t), p_{c,i}^y(t), p_{c,i}^z(t)]^\top \in \mathbb{R}^3$ can be obtained by:

$$\mathbf{p}_{c,i}(t) = \mathbf{R}_i^\top(t_{c,i})(\mathbf{p}_i(t) - \mathbf{p}_i(t_{c,i}))$$

For an object with known stiffness matrix $K_o \in \mathbb{R}^{3\times3}$ the force applied by each finger to the object in the contact frame is:

$$\boldsymbol{\lambda}_i(t) = \begin{cases} K_o \mathbf{p}_{c,i}(t) & \text{if } p_{c,i}^x(t) > 0 \\ 0 & \text{otherwise} \end{cases}$$

where $\boldsymbol{\lambda}_i(t) = [\lambda_i^x(t), \lambda_i^y(t), \lambda_i^z(t)]^\top \in \mathbb{R}^3$ is the force vector in the contact frame C_i and $p_{c,i}^x(t)$ is the normal component of $\mathbf{p}_{c,i}(t)$.

An accurate hand kinematic and configuration parameters ($\boldsymbol{l}_i$, $\mathbf{R}_{0,i}$, and $\boldsymbol{d}_i$) improve the accuracy of the force estimation using MARG sensors. Furthermore, an appropriate calibration procedure reduces bias and noise, and decreases the force estimation error. Moreover, using a high sampling time for the sensors results in a lower delay in contact event detection, and improves the accuracy of the proposed approach. A precise model of the stiffness matrix of the manipulated object leads to a better estimation of the fingertip contact forces.

IV. SIMULATION RESULTS

In order to evaluate the robustness of the proposed approach, and to deeply investigate the effects of various error sources, simulation studies have been performed. We simulated the bone and joint structures of the anthropomorphic hand. A MARG is considered for the palm and all phalanges. The data provided by the MARGs (orientation w.r.t. global frame) is used to reproduce the hand articulation pose. Contact event signals for each fingertip are simulated, so at the contact event time instances, the signal is logically high, and in all other moments it is logically low (similar to the real system). Simulations have been done in Simulink® using SimMechanics™ with a sampling time of 1 ms.

The simulation scenario is as follows. The deformable manipulated object is a sphere with 6 cm radius, and stiffness matrix $K_o = diag[1000, 1000, 1000]$ (N/m), initially located at $[50, -30, -70]$ mm w.r.t. palm. In the first five seconds the palm is fixed and the fingers approaching the object in a synergistic manner, each finger establishes a contact in different times ($t \in [0 \quad 5)$) while grasping the object; then, in next five seconds ($t \in [5 \quad 10)$) the fingers keep the contacts and the palm starts to rotate around its y-axis with a constant velocity up to 60 deg. In the next five seconds ($t \in [10 \quad 15)$) the palm goes back to its initial orientation while the fingers do not move. In the last five seconds ($t \in [15 \quad 20)$) the palm is fixed while the fingers are releasing the object in a synergistic manner.

TABLE I
HAND PARAMETERS AND PALM CONFIGURATION VALUES

hand parameters	nominal values	real values
l_1 (mm)	[40, 30, 28]	[40.29, 27.40, 21.60]
l_2 (mm)	[37, 24, 23]	[35.95, 24.96, 27.96]
d_1 (mm)	[20, 0, 0]	[13.55, 0, 0]
d_2 (mm)	[18.12, 67.61, 0]	[18.04, 67.34, 0]
$\mathbf{R}_{0,1}$	$\mathbf{I}_3$	$\mathbf{I}_3$
$\mathbf{R}_{0,2}$	$\mathbf{I}_3$	$\mathbf{I}_3$

TABLE II
NUMERICAL VALUES OF THE ERROR SOURCES USED FOR SIMULATION

Error source	values
Delay in contact detection (ms)	30
Error in link lengths $\boldsymbol{l}_i$ (mm)	$N(0, 5)$
Error in hand configuration parameter $\boldsymbol{d}_i$ (mm)	$N(0, 5)$
Bias of MARGs' orientation for each angle (deg)	$N(0, 2)$
Noise of MARGs' orientation for each angle (deg)	$N(0, 0.5)$
Stiffness matrix (N/m)	0

Fig. 4 shows a typical result of the algorithm including: joint angles $\boldsymbol{\theta}_i(t)$, fingertip positions w.r.t. the palm $\mathbf{p}_i(t)$, fingertip position w.r.t. contact frames $\mathbf{p}_{c,i}(t)$, contact event signals $\alpha_i(t)$, and estimated force vectors w.r.t. contact frames $\boldsymbol{\lambda}_i(t)$ for the thumb and index fingers. For the results presented in Fig. 4 the nominal values of the hand parameters and the palm configuration along with their real values are presented in Table I and a realistic set of values is considered for the different source of errors as shown in Table II.

The joint angles reconstruction is independent from link lengths $\boldsymbol{l}_i$, $\boldsymbol{d}_i$, and bias error of the MARGs, and as it can be seen from Fig. 4 it is less affected than the other variable. In Fig. 4(e)-(h) it is evident that once each contact event signal is triggered, the corresponding contact frame is created and
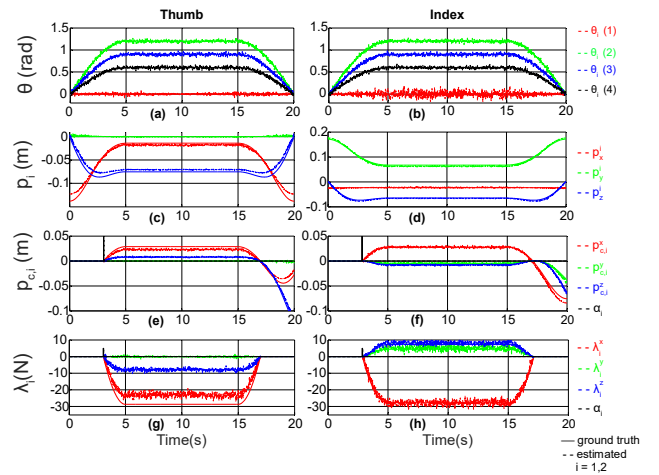

Fig. 4. Simulation results of hand tracking and fingertip contact force estimation in object manipulation for thumb and index finger: (a),(b) joint angles; (c),(d) fingertip positions w.r.t. palm; (e),(f) fingertip position w.r.t. contact frames and contact event signal; (g),(h) estimated fingertip contact forces.
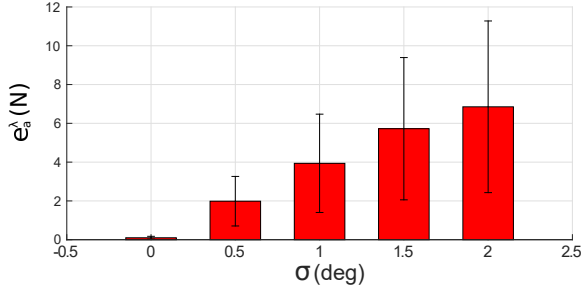
Fig. 5. Average and standard deviation of norm of contact force estimation error of all fingertips for different standard deviation σ of MARGs measurement noise.
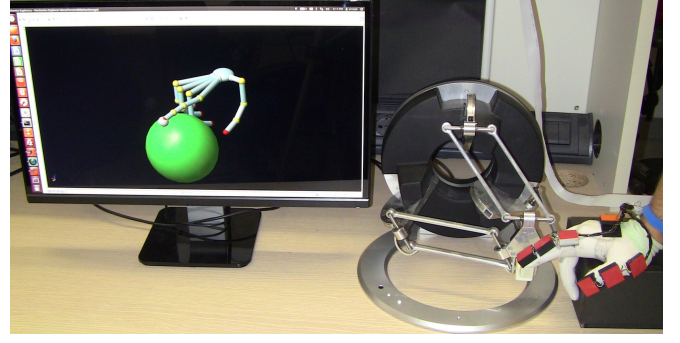

Fig. 6. Experimental setup: the subject wears the glove and manipulates a virtual object using index finger. The ground truth data is provided by the haptic device.

as far as the normal component of the fingertip position w.r.t. contact frame is positive, the force is estimated. As soon as the normal component of any fingertip position w.r.t. its corresponding contact frame become negative (the finger pad goes off the object) the force become zero.

The accuracy of the estimated forces depends on the precision of the hand model and on the accuracy of the MARGs measurements. We use the relative and absolute error criteria to evaluate the accuracy of different estimated signals. The relative error is defined as $e_r^{\boldsymbol{f}}(k) = \|\boldsymbol{f}_g(k) - \boldsymbol{f}(k)\|/\|\boldsymbol{f}_g(k)\|$, while the absolute error is $e_a^{\boldsymbol{f}}(k) = \|\boldsymbol{f}(k) - \boldsymbol{f}_g(k)\|$ where $\boldsymbol{f}(k)$ and $\boldsymbol{f}_g(k)$ are the estimated and ground truth vector signals, e.g., position and force, at the sampling time k, and $\|\|$ is the Euclidean norm. The accuracy of the estimated forces presented in Fig. 4(g),(h) for thumb is different from index finger, in fact $e_r^{\lambda(1)} = 20.56\%$, while $e_r^{\lambda(2)} = 4.95\%$ for the same level of measurement noise. The motivation is that the error of hand parameters and palm configuration of thumb is higher than index finger (see Table I).

In order to investigate the effect of measurement noise (assuming no bias error of the MARGs, delay in contact event detection, and error in stiffness matrix) we considered a Gaussian noise for MARGs' measurement error with zero mean and five different standard deviation ($\sigma = [0, 0.5, 1, 1.5, 2]$ deg). The simulation was performed 35 times for each different level of noise. Fig. 5 shows the average and standard deviation of $e_a^{\boldsymbol{\lambda}}$, during the simulation time for all the trials, in which $\boldsymbol{\lambda}$ is the concatenated vector containing all the estimated force vectors. As it can be seen the average and standard deviation of $e_a^{\boldsymbol{\lambda}}$ increase linearly with the standard deviation of MARGs measurement error.

V. EXPERIMENTAL VALIDATION

In order to validate the proposed approach, a set of experiments have been performed. Subjects wore the glove equipped with inertial and magnetic sensors on the palm, index and thumb finger. Their index finger was fixed on the handle of an omega.3 haptic device. The task was to touch, push, and release a virtual deformable object (Fig. 6). The virtual object was a sphere with 80 mm diameter with stiffness matrix $K_o = diag\{100, 100, 100\}$ (N/m) and it was

TABLE III
ERROR CRITERIA FOR POSITION AND FORCE ESTIMATION IN THE
EXPERIMENTAL VALIDATION

Error	position ($\boldsymbol{p}$)	force ($\boldsymbol{\lambda}$)
$avg(e_a)$	23 mm	1.04 N
$max(e_a)$	81 mm	6.38 N
$avg(e_r)$	4.17%	17.81%

positioned at [-30, 170, -80] (mm) w.r.t. palm. The gravity compensation of the haptic device was activated. For the present prototype of the system we used a sampling time of 50 ms. Data acquisition, visualization, and haptic rendering are all performed in Simulink® environment via C++ level 2 S-Functions (system-functions).

A typical result of the experiments is depicted in Fig. 7. The hand parameters and palm configuration values of the subject ($\boldsymbol{l}_2$, $\boldsymbol{d}_2$, and $\mathbf{R}_{0,2}$) are reported in Table I. Fig. 7(a) shows the joint angles of the index finger, Fig. 7(b) shows the position of the index fingertip w.r.t. palm obtained by the haptic device and the glove, Fig. 7(c) illustrates the position of index fingertip w.r.t. contact frames, and Fig. 7(d) shows the estimated forces by the haptic device and the glove. The estimated contact forces by the omega.3 are computed w.r.t. the palm and for the sake of comparison have been reported in the contact frames (see Fig. 7(d)). The contact event signal is depicted in all plots in order to clarify the state of the system during the contact event time instances.

For the results presented in Fig. 7(d) the average of e_a^{λ} is 1.04 N, its maximum is 6.38 N, and the average of relative error e_r^{λ} is 17.81%. For the results presented in Fig. 7(b), the average of e_a^p is 23 mm with the maximum of 81 mm, and the relative error e_r^p in percentage is 4.17%. The experimental results, summarized in Table III, show an acceptable performance of the proposed approach.

VI. CONCLUSION AND FUTURE WORK

In this paper we presented a new method to estimate the fingertip contact forces using inertial and magnetic sensors. No force sensor was used. Contact event detection was performed by monitoring the data from the accelerometers and gyroscopes placed on the distal phalanges of the hand.
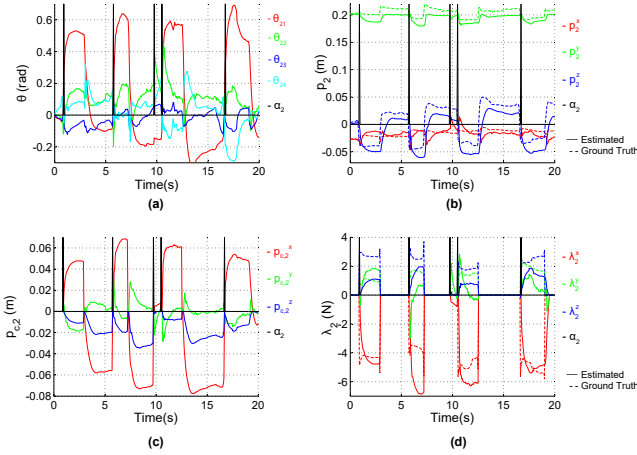
Fig. 7. Experimental results of hand tracking and fingertip contact force estimation in manipulating a virtual object with index finger, and comparison with ground truth data of the haptic device: (a) joint angles; (b) fingertip positions w.r.t. palm; (c) fingertip position w.r.t. contact frames; (d) estimated fingertip contact forces. The contact event signal is depicted in all plots in order to clarify the state of the system during the contact event time instances.

The kinematic model of the hand is used to estimate the fingertips' positions. For a deformable object with known stiffness matrix, the estimated force is obtained by multiplying the position of the fingertips in the contact frames and stiffness matrix of the object.

In future works, we will validate the proposed technique with real objects. Additional studies will be performed in order to relax the constraints used in this work and make the proposed method more general.

REFERENCES

[1] R. Johansson and A. B. Vallbo. Skin mechanoreceptors in the human hand: An inference of some population. *Sensory Functions of the Skin in Primates: With Special Reference to Man*, 27:171, 2014.

[2] Po-Tsun Chen, I-Ming Jou, Chien-Ju Lin, Hsiao-Feng Chieh, Li-Chieh Kuo, and Fong-Chin Su. Is the control of applied digital forces during natural five-digit grasping affected by carpal tunnel syndrome? *Clinical Orthopaedics and Related Research®*, 473(7):2371–2382, 2015.

[3] H. C. Fischer, K. Stubblefield, T. Kline, X. Luo, R. V. Kenyon, and D. G. Kamper. Hand rehabilitation following stroke: a pilot study of assisted finger extension training in a virtual environment. *Topics in Stroke Rehabilitation*, 14(1):1–12, 2007.

[4] M. A. Otaduy, C. Garre, and M. C. Lin. Representations and algorithms for force-feedback display. *Proceedings of the IEEE*, 101(9):2068–2080, 2013.

[5] A. M. Dollar, A. Bicchi, M. R. Cutkosky, and R. D. Howe. Special issue on the mechanics and design of robotic hands. *The International Journal of Robotics Research*, 33(5):675–676, 2014.

[6] K. Kronander and A. Billard. Learning compliant manipulation through kinesthetic and tactile human-robot interaction. *Haptics, IEEE Transactions on*, 7(3):367–380, 2014.

[7] J. Vogel, S. Haddadin, B. Jarosiewicz, J. D. Simeral, D. Bacher, L. R. Hochberg, J. P. Donoghue, and P. Van Der Smagt. An assistive decision-and-control architecture for force-sensitive hand–arm systems driven by human–machine interfaces. *The International Journal of Robotics Research*, 34(6):763–780, 2015.

[8] E. Battaglia, M. Bianchi, A. Altobelli, G. Grioli, M. Catalano, A. Serio, M. Santello, and A. Bicchi. Thimblesense: a fingertip-wearable tactile sensor for grasp analysis. *Haptics, IEEE Transactions on*, PP(99):1–1, 2015.

[9] Jilin Zhou, F. Malric, and S. Shirmohammadi. A new hand-measurement method to simplify calibration in cyberglove-based virtual rehabilitation. *Instrumentation and Measurement, IEEE Transactions on*, 59(10):2496–2504, 2010.

[10] G. H. Büscher, R. Kõiva, C. Schürmann, R. Haschke, and H. J. Ritter. Flexible and stretchable fabric-based tactile sensor. *Robotics and Autonomous Systems*, 63:244–252, 2015.

[11] M. Bianchi, N. Carbonaro, E. Battaglia, F. Lorussi, A. Bicchi, D. De Rossi, and A. Tognetti. Exploiting hand kinematic synergies and wearable under-sensing for hand functional grasp recognition. In *Wireless Mobile Communication and Healthcare (Mobihealth), 2014 EAI 4th International Conference on*, pages 168–171, 2014.

[12] S. Mascaro and H. H. Asada. Photoplethysmograph fingernail sensors for measuring finger forces without haptic obstruction. *Robotics and Automation, IEEE Transactions on*, 17(5):698–708, 2001.

[13] S. Mascaro and H. H. Asada. Measurement of finger posture and three-axis fingertip touch force using fingernail sensors. *Robotics and Automation, IEEE Transactions on*, 20(1):26–35, 2004.

[14] Y. Sun, J. M. Hollerbach, and S. Mascaro. Predicting fingertip forces by imaging coloration changes in the fingernail and surrounding skin. *Biomedical Engineering, IEEE Transactions on*, 55(10):2363–2371, 2008.

[15] Z. Ju and H. Liu. Human hand motion analysis with multisensory information. *Mechatronics, IEEE/ASME Transactions on*, 19(2):456–466, 2014.

[16] P. G. Kry and D. K. Pai. Interaction capture and synthesis. In *ACM Transactions on Graphics (TOG)*, volume 25, pages 872–880, 2006.

[17] Tu-Hoa Pham, A. Kheddar, A. Qammaz, and A.A. Argyros. Towards force sensing from vision: Observing hand-object interactions to infer manipulation forces. In *Computer Vision and Pattern Recognition (CVPR), 2015 IEEE Conference on*, pages 2810–2819, 2015.

[18] Marco Fontana, Simone Marcheschi, Fabio Salsedo, and Massimo Bergamasco. A three-axis force sensor for dual finger haptic interfaces. *Sensors*, 12(10):13598–13616, 2012.

[19] H. G. Kortier, V. I. Sluiter, D. Roetenberg, and P. H. Veltink. Assessment of hand kinematics using inertial and magnetic sensors. *Journal of Neuroengineering and Rehabilitation*, 11(1):70, 2014.

[20] T. Lisini Baldi, M. Mohammadi, S. Scheggi, and D. Prattichizzo. Using inertial and magnetic sensors for hand tracking and rendering in wearable haptics. In *World Haptics Conference (WHC), 2015 IEEE*, pages 381–387, 2015.

[21] D. Comotti. Orientation estimation based on gauss-newton method and implementation of a quaternion complementary filter, 2011.